



ELSEVIER

Contents lists available at SciVerse ScienceDirect

Talanta

journal homepage: www.elsevier.com/locate/talanta

Complexation of Hg(II) by humic acid studied by square wave stripping voltammetry at screen-printed gold electrodes

Fernando Henrique do Nascimento, Jorge Cesar Masini*

Instituto de Química, Universidade C.P. 26077, 05513-970 São Paulo, Brazil

ARTICLE INFO

Article history:

Received 5 July 2012

Received in revised form

7 August 2012

Accepted 14 August 2012

Available online 23 August 2012

Keywords:

Mercury

Dynamic speciation

Humic acid

Sequential injection analysis

Voltammetry

ABSTRACT

This paper reports the development of a sequential injection (SI) method to study the complexation of Hg(II) by humic acid (HA) using square wave anodic stripping voltammetry at a screen-printed gold electrode (SPGE). The SI system injected samples (in 0.020 mol L⁻¹ NaNO₃ and pH 6.0) to the flow cell during the deposition step and exchanged the medium to 0.050 mol L⁻¹ HCl to perform the stripping step under stopped flow conditions. For sample volume=750 μL, flow rate=15 μL s⁻¹ (deposition step), and square wave frequency=100 Hz, the detection limit was 20 nmol L⁻¹ and the sampling throughput was 17 analyses per hour. Complexation of Hg(II) was studied using a 25.0 mg L⁻¹ suspension of HA (72.5 μmol L⁻¹ of ionizable sites), and total Hg(II) concentrations from 1 to 20 μmol L⁻¹. The diffusion coefficient of the complex was $(1.3 \pm 0.2) \times 10^{-7}$ cm² s⁻¹. A complexing capacity of 537 μmol g⁻¹ was found. The log of the differential stability constant (log K_{DEF}) decreased from 7.0 to 5.3 as the log of the degree of site occupation (log θ) increased from -1.6 to -0.5. The values of log K_{DEF} were consistent with complexation of Hg(II) by carboxylic and phenolic groups.

© 2012 Elsevier B.V. All rights reserved.

1. Introduction

Complexation of Hg(II) by humic substances play an important role in controlling the reactivity and geochemical transport of Hg in soil and aquatic environments. The understanding of Hg(II) biogeochemistry has been hampered by a lack of reliable data describing the strength of the binding of Hg(II) by humic and fulvic acids, as well as other constituents of the dissolved organic matter (DOM) [1]. The difficulty in obtaining these data is caused by the intrinsic complexity of humics, which are consisted of heterogeneous supramolecular structures containing a variety of potential metal binding sites whose central atom is usually O, N or S [1,2]. Nitrogen and sulfur form the strong binding sites that govern the free concentration of Hg(II) under conditions of low loading of the metal species. However, binding sites containing N and S are much less abundant than those containing O (carboxylic and phenolic), which form weak complexes with Hg(II) and control the free concentration under conditions of high loading of the metal ion (polluted environments) [3,4].

Stability constants of the interaction Hg(II)–DOM have been determined by techniques such as potentiometric titration using iodide ion-selective electrodes [5], anodic stripping voltammetry [6], competitive complexation with Br⁻ [7], fluorescence

spectroscopy [8,9], reducible-Hg titrations [10] and equilibrium dialysis [3]. Gasper et al. [1] published a critical review on three methods based on ion exchange, liquid–liquid extraction with competitive ligand exchange and solid-phase extraction with competitive ligand exchange. Cold vapor atomic absorption spectrometry (CVAAS) or cold vapor atomic fluorescence spectrometry (CVAFS) was used for determination of the Hg(II) concentrations [1]. Some of these techniques [1,3,7,10] are laborious, requiring extensive sample handling and separation steps. The stability constants represent a weighted average of binding strengths of the sites at a given metal to ligand ratio [11].

A voltammetric sensor for dynamic speciation is characterized by its response time, which is determined by the thickness of the diffusion layer, and the accumulation time, which is the length of time over which the metal species are accumulated in the working electrode prior to quantification. The signal resulting from the accumulation step represents an integration of all fluctuations in the test medium during this time period [12]. At our best knowledge, only one study of the Hg(II) binding by DOM using stripping voltammetry has been published [6]. In that work the accumulation step was made in buffered medium (pH 7.2) which was manually exchanged to a mixture of 0.10 mol L⁻¹ HClO₄ and 2.5 mmol L⁻¹ HCl for the stripping step. Flow methods of analysis, especially sequential injection analysis [13], are known to provide very reproducible flow patterns, which determine the thickness of the diffusion layer, leading to highly reproducible conditions of mass transport toward the electrode surface [14–16]. Besides, medium

* Corresponding author. Tel.: +55 11 3091 1469; fax: +55 11 3855 5579.
E-mail addresses: jcmasini@iq.usp.br, jcmasini@gmail.com (J.C. Masini).

exchange strategies are easily implemented in flow methods, minimizing the errors due to differences in electrode positioning and metal oxidation during the exposition of the electrode to the atmosphere [17,18]. Despite of these interesting features, SI methodologies have not yet been explored for dynamic speciation studies.

Progresses in screen-printed technologies along the last decades [19] led to the development of robust screen-printed electrodes (SPE) which have found extensive application as low cost sensors suitable field measurements and environmental monitoring [20]. As SIA systems, SPEs have been underutilized in speciation studies in environmental matrices. In the present paper a SI procedure was developed for determination of mean diffusion coefficients, mean stability constant, differential equilibrium function, and binding capacity parameters related to complexation of Hg(II) by carboxylic and phenolic groups of a commercial HA using square wave voltammetry and Screen-Printed Gold Electrodes (SPGE).

2. Experimental

2.1. Reagents and apparatus

All reagents were of analytical grade from Merck (Darmstadt, Germany) or Sigma-Aldrich (St. Louis, MO, USA). Solutions were prepared using distilled and deionized water ($> 18 \text{ M}\Omega \text{ cm}$ resistivity) obtained from a Simplicity 185 system from Millipore (Billerica, MA, USA) coupled to an UV lamp. Stock and working solutions were: 0.20 and $1.0 \text{ mol L}^{-1} \text{ NaNO}_3$ (Merck), $0.050 \text{ mol L}^{-1} \text{ HCl}$ (Merck), 0.10 and $1.0 \text{ mol L}^{-1} \text{ HNO}_3$ (Merck), 1000 mg L^{-1} standard stock Hg(II) in $10\% (\text{v v}^{-1}) \text{ HNO}_3$ (Merck), 1.0 and 0.100 g L^{-1} sodium salt of humic acid from Sigma-Aldrich (Lot STBB 1688).

Voltammetric measurements were carried out in a PalmSens potentiostat (Palm Instrument BV, Houten, The Netherlands) using the PSTrace 2.4 software for instrument control and data acquisition. The flow cell was assembled using "University of Florence" Screen Printed Sensor made of a gold working electrode (area of 7.06 mm^2 and thickness of $450 \mu\text{m}$), an Ag pseudo-reference and a graphite counter electrode [21]. Solution handling was carried out using a FIALab 3500 (FIALab Instruments, Bellevue, WA) according to Fig. 1. Solutions were driven by a 5.00 mL Cavro syringe pump, SP (Cavro Scientific Instruments, Sunnyvale, CA) and an eight port rotary valve, RV (Valco Instrument Co., Houston, TX). The syringe pump and the rotary valve were connected through a three-way valve, SV (Positions IN and OUT), by the holding coil, HC, which was made of 3 m of 0.8 mm i.d. Teflon (PolyTetraFluoroEthylene, PTFE) tubing. Connections of the

solutions and detector cell with the rotary valve were made of 0.5 mm i.d. PTFE tubing and PTFE nuts and ferrules (Upchurch, Oak Harbor, WA). The control of the pump and valve was made with the FIALab 5.0 software.

2.2. Sequential injection procedure

The SI system is schematized in Fig. 1 and the procedure to determine the free/labile Hg(II) concentrations is described in Table 1. First of all the tubing connecting the carrier reservoir to the flow cell was filled with carrier solution ($0.050 \text{ mol L}^{-1} \text{ HCl}$). Tubing connecting ports 1 and 3 of RV were filled with sample solution and $0.020 \text{ mol L}^{-1} \text{ NaNO}_3$ at pH 6.0, respectively. Tubing connected to port 7 was left empty, open to air. Before starting a new analysis, the tubing connecting RV to the sample reservoir was washed with the solution to be analyzed. The analysis cycle (Table 1) started by aspirating $2500 \mu\text{L}$ of carrier (C) solution into the syringe (S), followed by injection of $1000 \mu\text{L}$ of C in the flow cell while the potentiostat applied a conditioning potential of 0.7 V between working and reference electrodes (Steps 1 to 6). An air bubble was aspirated into HC (Steps 7 and 8). The solution inside the flow cell was changed to the $0.020 \text{ mol L}^{-1} \text{ NaNO}_3$ at pH 6.0 solution (Steps 9–12). While these steps were done, the potential of 0.7 V remained applied to the electrodes. The sample volume was aspirated into HC (step 13–14) and, during this operation the potentiostat applied the deposition potential of 0.3 V (Step 15). A defined volume of sample was injected to the flow cell at a constant flow rate (steps 16 and 17), keeping the air bubble inside the HC. The air bubble was eliminated from the system through port 4 of RV (Steps 18 and 19). Carrier solution was pumped toward the flow cell performing the medium exchange (Steps 20 and 21). The flow was stopped and the potentiostat scanned the potential from 0.3 to 0.7 V at a square wave frequency of 100 Hz , pulse step of 0.006 V and pulse amplitude of 0.04 V (Steps 22 and 23), reoxidizing the deposited Hg^0 . Finally the syringe was emptied, flushing out the flow cell with $0.050 \text{ mol L}^{-1} \text{ HCl}$ solution (Step 24).

2.3. Titration of HA with Hg(II)

These experiments were made using stock solutions of $100 \text{ mg L}^{-1} \text{ HA}$, $1.0 \text{ mol L}^{-1} \text{ NaNO}_3$ and 20 or $200 \mu\text{mol L}^{-1} \text{ Hg(II)}$, all of them conditioned at $\text{pH } 6.0 \pm 0.1$. The experiments were made in nine polypropylene centrifuge tubes (Corning™) with capacity of 15 mL , previously treated with $10\% (\text{v v}^{-1}) \text{ HNO}_3$ followed by extensive washing with deionized water. To each tube 2.50 mL of the $100 \text{ mg L}^{-1} \text{ HA}$ solution was added, followed by $200 \mu\text{L}$ of the $1.0 \text{ mol L}^{-1} \text{ NaNO}_3$ solution and suitable volumes of the stock Hg(II) solutions to generate total Hg(II) concentrations between 1.0 and $20.0 \mu\text{mol L}^{-1}$ and $0.020 \text{ mol L}^{-1} \text{ NaNO}_3$ at $\text{pH } 6.0 \pm 0.1$ after dilution to 10.0 mL with deionized water. The tubes were agitated at 180 rpm in an orbital shaker (Marconi Model MA-832) thermostated at $25.0 \pm 0.5 \text{ }^\circ\text{C}$ for 2 h . Next, HA suspensions were directly analyzed by the SIA system before and after filtration in Minisart® syringe filters from Sartorius with $0.20 \mu\text{m}$ porosity and 28 mm membrane diameter. To correct for any adsorption onto polypropylene or Teflon tubing, the calibration was made with Hg(II) standard solutions (in $0.010 \text{ mol L}^{-1} \text{ NaNO}_3$ at $\text{pH } 6.0$) that passed by similar treatments as those in presence of HA.

2.4. Data treatment

The peak current (i_p) in non-complexing medium ($0.020 \text{ mol L}^{-1} \text{ NaNO}_3$) is given by

$$i_p = BD_{\text{Hg}}^p C_{\text{Hg},T} \quad (1)$$

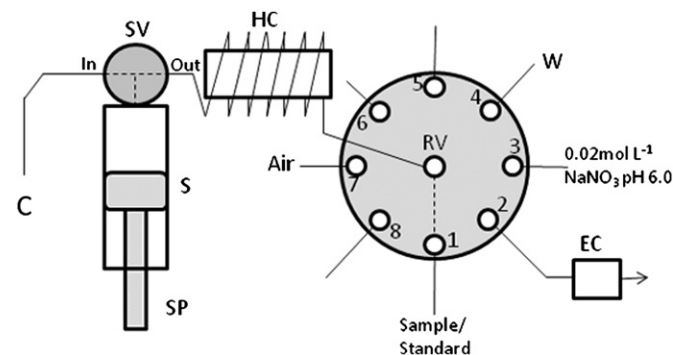


Fig. 1. Sequential injection system for Hg(II) dynamic speciation by square wave stripping voltammetry. C=carrier, composed of $0.05 \text{ mol L}^{-1} \text{ HCl}$; SV=3-way syringe valve (positions In and Out); S=syringe; SP=Syringe Pump; HC=Holding Coil (3 m of 0.8 mm i.d. PTFE tubing); RV=Rotary Selection Valve; EC=Electrochemical Flow Cell; W=Waste.

Table 1

Sequence of operations to perform automated medium exchange and electrochemical determination of free/labile fraction of Hg(II) by SIA.

Step	Component	Command	Parameter/Position	Comment
1	EC		0.7 V for 75 s	Applying conditioning potential
2	SV	Commute	In	
3	SP	Aspirate	2500 μL at 200 $\mu\text{L s}^{-1}$	Aspirating carrier into the syringe
4	SV	Commute	Out	
5	RV	Commute	Port 2	
6	SP	Dispense	1000 μL at 100 $\mu\text{L s}^{-1}$	Electrochemical conditioning and cell cleaning
7	RV	Commute	Port 7	
8	SP	Aspirate	100 μL at 50 $\mu\text{L s}^{-1}$	Aspirating air bubble into HC
9	RV	Commute	Port 3	
10	SP	Aspirate	500 μL at 100 $\mu\text{L s}^{-1}$	Aspirating 0.02 mol L ⁻¹ NaNO ₃ at pH 6.0 into HC
11	RV	Commute	Port 2	
12	SP	Dispense	300 μL at 100 $\mu\text{L s}^{-1}$	Filling EC with 0.02 mol L ⁻¹ NaNO ₃
13	RV	Commute	Port 1	
14	SP	Aspirate	250 μL^a at 50 $\mu\text{L s}^{-1}$	Aspirating sample into HC
15	EC		0.3 V for 32 s	Applying deposition potential
16	RV	Commute	Port 2	
17	SP	Dispense	225 μL^a at 30 $\mu\text{L s}^{-1}$	Injecting sample into EC
18	RV	Commute	Port 4	
19	SP	Dispense	800 μL at 200 $\mu\text{L s}^{-1}$	Discarding air bubble
20	RV	Commute	Port 2	
21	SP	Dispense	250 μL at 50 $\mu\text{L s}^{-1}$	Performing medium exchange
22	SP	Stop	10 s	Stopping the flow for the stripping step
23	EC		Scan 0.3 to 0.7 V, 100 Hz, pulse height 0.04 V	Hg reoxidation in 0.05 mol L ⁻¹ HCl
24	SP	Empty	200 $\mu\text{L s}^{-1}$	Emptying the syringe to finish the analysis

^a Volumes used to extend the linear response up to 10 $\mu\text{mol L}^{-1}$.

where D_{Hg} =diffusion coefficient of Hg(II), estimated as $9.2 \times 10^{-6} \text{ cm}^2 \text{ s}^{-1}$ by Danwanichakul and Danwanichakul [22]; p =empirical constant whose value varies between 1/2 and 2/3 [23] (1/2 was adopted in the present work). $C_{\text{Hg},T}$ =total concentration of Hg(II); B =constant dependent on the flow rate, electrode area, deposition time, and the number of electrons involved in the electrode reaction. The value of B was estimated from the slope of the calibration curve in non-complexing medium.

In the complexing medium containing HA the diffusion coefficient must be substituted by a mean value for each $C_{\text{Hg},T}$ because not only the free species is reduced at the electrode, but also the labile fraction of complexed cations in the diffusion layer [23]. As HAs are constituted by supramolecular self-assembled structures [2], their complexes of Hg(II) diffuse slower than the free ion (or complexes involving simple structures such as those involved in hydroxides, chloride, etc). Thus, in a medium containing HA at similar pH and ionic strength as those used in the calibration in the non-complexing medium (0.020 mol L⁻¹ NaNO₃ and pH 6.0), and assuming the complexes are labile, the Eq. (1) can be rewritten as:

$$i_p^L = B\bar{D}^p C_{\text{Hg},T} \quad (2)$$

where i_p^L is the peak current in presence of HA and \bar{D} is the mean diffusion coefficient, which can be obtained from the

$$\frac{i_p^L}{i_p} = \left(\frac{\bar{D}}{D_{\text{Hg}}} \right)^{1/2} \quad (3)$$

The value of \bar{D} is pondered by its relative proportion to $C_{\text{Hg},T}$ according to Eq. (4) [23]:

$$\bar{D} = \frac{D_{\text{Hg}}C_{\text{Hg}} + D_{\text{Hg}L}C_{\text{Hg}L}}{C_{\text{Hg},T}} \quad (4)$$

where C_{Hg} is the concentration of free Hg(II), $C_{\text{Hg}L}$ =concentration of complexed Hg(II) at the equilibrium; $D_{\text{Hg}L}$ =Diffusion coefficient for the Hg_L complex, whose value can be estimated from the slope of the first points of the titration of HA with Hg(II), a situation in which the concentration of free Hg(II) is not significant for the peak current (low $C_{\text{Hg},T}$, low degree of site

occupation) [23,24]. The term B (Eq. (1)) was used for computation of $D_{\text{Hg}L}$. This strategy is favored by the highly reproducible flow patterns provided by the SI system, leading to very reproducible mass transport, given that all other conditions such as electrode, number of electrons involved, temperature, pH and ionic strength are the same in both complexing and non-complexing media. Using this approach, a $D_{\text{Hg}L} = (1.3 \pm 0.2) \times 10^{-7} \text{ cm}^2 \text{ s}^{-1}$ was obtained and substituted in Eq. (4) to compute C_{Hg} along the titration curve. The values of $C_{\text{Hg}L}$ were obtained from the mass balance:

$$C_{\text{Hg}L} = C_{\text{Hg},T} - C_{\text{Hg}} \quad (5)$$

Data was initially fitted to classic Langmuir and Freundlich isotherms (Eqs. (6) and (7), respectively):

$$Q = \frac{Q_{\text{max}}K_L C_{\text{Hg}}}{1 + K_L C_{\text{Hg}}} \quad (6)$$

$$Q = K_f C_{\text{Hg}}^{1/n} \quad (7)$$

where Q is the amount of Hg(II) adsorbed per unit mass of HA (mol g⁻¹), Q_{max} is the maximum capacity of adsorption, K_L is the Langmuir free energy term related to adsorption (L mol⁻¹), K_f is the Freundlich capacity constant and $1/n$ is an empirical parameter related to the energetic heterogeneity of the adsorption sites, with values between 0 (totally heterogeneous) and 1 (completely homogeneous).

The average equilibrium constant, \bar{K} , and the differential equilibrium function, K_{DEF} , were calculated as described by Pinheiro et al. [23] and Bugarin et al. [25]. The \bar{K} value was calculated according to the

$$\bar{K} = \frac{\sum_j^n C_{\text{Hg}L}}{C_{\text{Hg}} \sum_j^n C_{L,j}} \quad (8)$$

where L_j is the complexing site j in the HA, n is the total number of complexing sites and $C_{L,j}$ is the equilibrium concentration of the not complexed site j , which can be computed from the mass balance:

$$\sum_j C_{L,j} = C_{L,T} - \sum_j C_{MLj} \quad (9)$$

$C_{L,T}$ is the total concentration of ionizable sites obtained by potentiometric titration with NaOH, followed by data treatment using linearization of the titration curve by modified Gran functions [26,27].

Computation of K_{DEF} was made with equation [23,28]:

$$K_{DEF} = -\frac{\alpha^2}{C_{Hg,T}} \left[\frac{1}{1 + (\alpha - 1) \left(\frac{d \ln C_{Hg,T}}{d \ln z} \right)} \right] \quad (10)$$

where $\alpha = C_{Hg,T}/C_{Hg}$. The differential term was obtained by fitting a polynomial function to data plotted as $\ln C_{Hg,T}$ as a function of $\ln \alpha$.

The degree of site occupation was computed as the ratio $\theta = C_{HgI}/C_{L,T}$. According to Eq. (11), a plot of $\log \theta$ vs. $\log K_{DEF}$ gives the heterogeneity parameter, Γ , and K_{DEF}^0 , which is the K_{DEF} for $\theta = 1$ [28]

$$\log \theta = \Gamma \log K_{DEF}^0 - \Gamma \log K_{DEF} \quad (11)$$

3. Results and discussion

3.1. Method development

Hydrochloric acid is commonly used as the supporting electrolyte for voltammetric determination of Hg(II) because the formation of Hg(II)-chlorocomplexes during the stripping step decreases the background current and enhances the sensitivity [29–32]. In the present work, 0.050 and 0.10 mol L⁻¹ HCl solutions were tested as supporting electrolyte in the stripping step. The 0.050 mol L⁻¹ solution provided low background currents and allowed to perform about 50 measurements before deterioration of the electrode response, whereas no more than 35 analyses were possible in 0.10 mol L⁻¹ HCl. Thus, the concentration of 0.050 mol L⁻¹ was used in the method. Activation of the SPGE was made under continuous flow conditions using the SI instrument to pump 5 mL of 0.050 mol L⁻¹ HCl solution at 20 $\mu\text{L s}^{-1}$ through the flow cell. Simultaneously, a conditioning potential of 0.70 V was applied for 15 s, followed by five cycles of cyclic voltammetry, scanning the potential from 0 to 0.7 V at a scan rate of 0.050 V s⁻¹ [32]. Before each analysis, electrochemical conditioning was made by applying a potential of 0.7 V for 75 s to the SPGE (in 0.05 mol L⁻¹ HCl) (steps 1 to 14, Table 1).

The amount of Hg deposited on the SPGE is directly related to the free Hg(II) concentration in bulk solution plus the labile fraction in the diffusion layer [24]. Both these fractions are influenced by hydrogen ion activity. Thus, the pH of the sample solution flowing through the cell during the deposition step cannot be altered in relation to the pH of the solution in which the complexation parameters are being determined. As the pH of the sample solutions are close to neutrality (to be representative of natural waters), these solutions cannot be dispersed with the 0.050 mol L⁻¹ HCl carrier solution during the deposition step. This was achieved by using the segmented flow approach, inserting an air bubble between the sample and the carrier solutions (step 8, Table 1) [33]. Besides, as the flow cell was filled with 0.050 mol L⁻¹ HCl in the beginning of each analysis, this solution had to be flushed with 300 μL of 0.020 mol L⁻¹ NaNO₃ (pH 6.0). This flushing was made by keeping the air bubble inside the holding coil of the SIA system (step 12, Table 1), so that in the next step of the procedure, when the sample solution was aspirated to the holding coil, there was no interdispersion between carrier and sample. All these operations were made with the conditioning potential of 0.7 V applied to the electrode. At the end of the sample aspiration step the potentiostat applied the deposition potential to the electrochemical cell.

The next step of the method development was the evaluation of the influence of flow rate, sample volume and square wave frequency on the oxidation peak currents. All these experiments were made at a deposition potential of 0.30 V vs. Ag/AgCl, which is adequate for reduction of Hg(II) [32], without interference of Cu(II), Pb(II), Cd(II), and other metal ions [35], conferring selectivity to the measurements. For a fixed sample volume of 1000 μL and frequency of 20 Hz, flow rates of 5, 10, 15 and 30 $\mu\text{L s}^{-1}$ were imposed to the solution during the deposition step, adjusting the time so that the deposition potential was applied while the sample solution was passing through the flow cell. Peak currents for a 1.0 $\mu\text{mol L}^{-1}$ Hg(II) solutions decreased systematically as the flow rate increased from 5 to 30 $\mu\text{L s}^{-1}$ (Fig. 2). This means that the more efficient mass transport expected at high flow rates did not compensate for the reduced contact time of the sample solution with the electrode surface. A flow rate of 5 $\mu\text{L s}^{-1}$ would be recommended to reach a maximum signal to noise ratio, but the decrease in flow rate from 15 to 5 $\mu\text{L s}^{-1}$ enhanced the peak current by only 15%, whereas the deposition time had to be increased from 70 to 200 s, causing a significant decrease in sampling throughput. Thus, a flow rate of 15 $\mu\text{L s}^{-1}$ was used as a compromise between sensitivity and rapidity of analysis.

Increase in sample volume increased the peak current, but a decrease in the slope was observed for volumes larger than 750 μL (Fig. 2). Thus, the sample volume of 750 μL was used in the optimized procedure. Peak currents increased with the square wave frequency up to 100 Hz (Fig. 2), so that this frequency was used in all further experiments.

3.2. Figures of merit

For the sample volume of 750 μL , flow rate of 15 $\mu\text{L s}^{-1}$ and square wave frequency of 100 Hz, peak currents (i_p) obey a linear relation with $C_{Hg,T}$ described by the equation $i_p = (0.51 \pm 0.01)C_{Hg,T} + (0.02 \pm 0.002)$ (Fig. 3), with $r^2 = 0.998$, for a concentration range between 0.050 and 0.50 $\mu\text{mol L}^{-1}$. Under these conditions the Limits of Detection and Quantification (LOD and LOQ) were 0.017 and 0.050 $\mu\text{mol L}^{-1}$, computed as $3.sd/S$ and $10.sd/S$, respectively, where sd is the standard deviation of 10 measurements of blank solution (0.02 mol L⁻¹ NaNO₃ adjusted to pH 6.0) and S is the slope of the calibration curve. The sampling throughput was 17 analyses per hour.

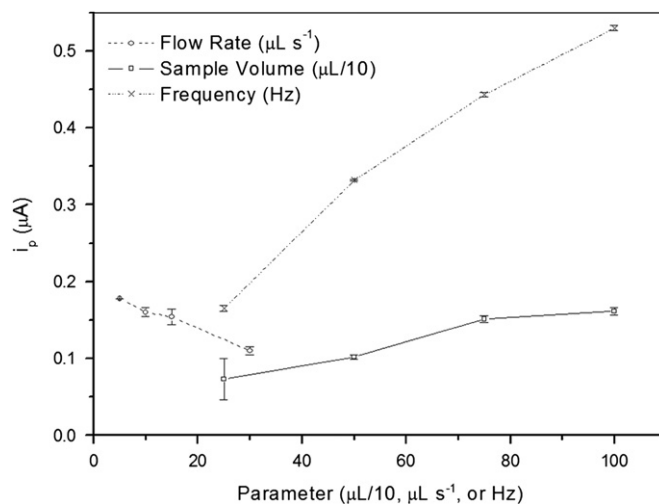


Fig. 2. Effect of flow rate, sample volume and square wave frequency on the peak current for Hg⁰ oxidation. Flow rate was studied at 20 Hz for a sample volume of 1000 μL ; Sample volume was studied at 20 Hz and flow rate of 15 $\mu\text{L s}^{-1}$; Frequency was studied at flow rate of 15 $\mu\text{L s}^{-1}$ using a sample volume of 1000 μL .

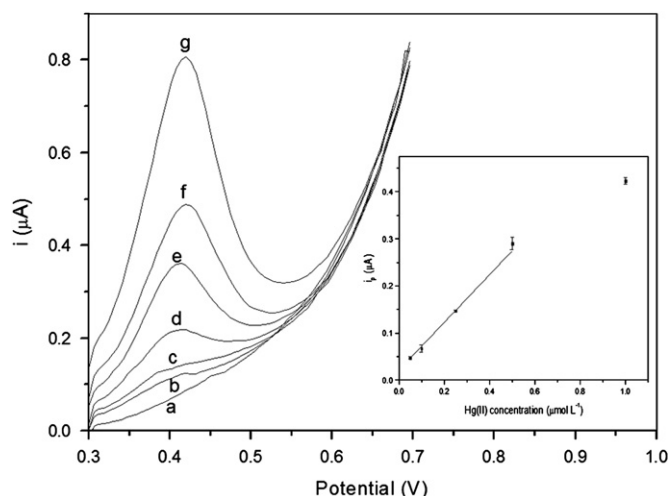


Fig. 3. Example of calibration curve in non-complexing medium ($0.020 \text{ mol L}^{-1} \text{ NaNO}_3$, pH 6.0) obtained by injecting $750 \mu\text{L}$ of sample at flow rate of $15 \mu\text{L s}^{-1}$ during the deposition time (deposition potential of 0.3 V) followed by square wave anodic stripping voltammetry at 100 Hz of frequency, pulse height of 0.040 V . Hg(II) concentrations are as follows: (a) blank; (b) 0.050 ; (c) 0.10 ; (d) 0.25 ; (e) 0.50 ; (f) 1.0 and (g) $2.5 \mu\text{mol L}^{-1}$. The inset shows the linear calibration range between 0.050 and $0.50 \mu\text{mol L}^{-1}$.

Dynamic speciation studies require sensitive analytical techniques to determine free/labile concentrations under low degree of site occupation (strongest sites). In addition, the technique should be sufficiently precise to characterize the weakest sites (small differences between total and free ion concentration) [34]. This feature requires wide a linear dynamic range. Some authors have reported wide ranges of linear response for determination of Hg(II) with gold film electrodes [35,36], or rotating disk gold electrodes [37]. Other authors, also using gold electrodes, have reported narrow linear dynamic ranges [30,38,39], not extending far from one decade of concentration, as observed in the present work. To overcome this limitation, the automated SIA system can make changes in the procedure (varying the sample volume or the flow rate, and, as a consequence, the deposition time) to explore different analytical windows and different degrees of site occupation. By decreasing the sample volume to $250 \mu\text{L}$ and increasing the flow rate to $30 \mu\text{L s}^{-1}$ (decreasing the deposition time to 32 s , experimental conditions described in Table 1), the linear dynamic range can be displaced from $0.05\text{--}0.50 \mu\text{mol L}^{-1}$ to $0.50\text{--}10 \mu\text{mol L}^{-1}$, allowing one to investigate the titration curve close to the region of site saturation. The mean slope and intercept of 5 calibration curves obtained in different working days and different SPGE were $0.43 \pm 0.01 \mu\text{A L } \mu\text{mol}^{-1}$ and $-0.11 \pm 0.04 \mu\text{A}$, respectively, implying in a relative standard deviation of 2.3% in slope and an intercept not statistically different from the zero value. Under these conditions the sampling throughput increased to $35 \text{ samples h}^{-1}$.

3.3. Test of electrode passivation and HA adsorption

To verify if the measurements in presence of HA passivate the gold electrode, a sequence of 4 injections of a $0.25 \mu\text{mol L}^{-1} \text{ Hg(II)}$ solution in non-complexing medium was made. Solutions of increasing $C_{\text{Hg},T}$ (1.0 , 4.0 and $8.0 \mu\text{mol L}^{-1}$) in presence of 25 mg L^{-1} of HA were injected between each one of the experiments carried out in non-complexing medium (Fig. 4). Peak potentials and peak currents in non-complexing media measured just after the experiments in presence of HA did not show any systematic variation, suggesting that there is no adsorption of HA on the gold surface. The measurements in presence of HA

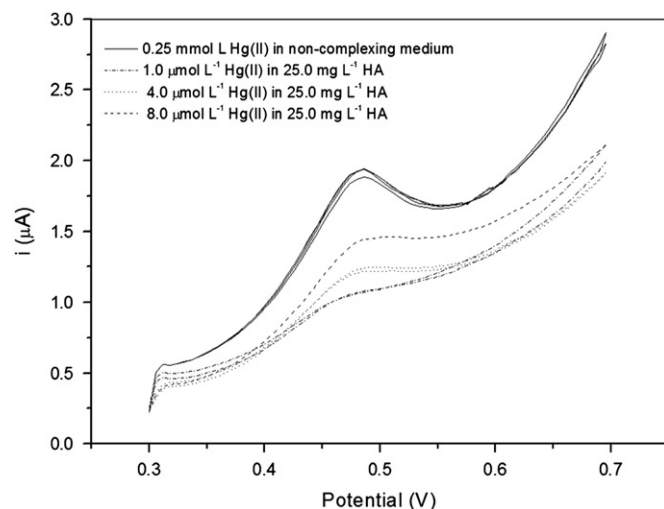


Fig. 4. Test of electrode passivation and memory effects made in presence and absence of HA, both in $0.020 \text{ mol L}^{-1} \text{ NaNO}_3$ at pH 6.0. The first measurement was made with the $0.25 \mu\text{mol L}^{-1} \text{ Hg(II)}$ solution in non-complexing medium. The other voltammograms were intercalated by measurements of solutions of increasing concentrations of Hg(II) in the complexing medium of HA.

Table 2

Concentration and pKa of ionizable sites determined in the humic acid sample by potentiometric titration in $0.020 \text{ mol L}^{-1} \text{ NaNO}_3$ and $25.0 \pm 0.1 \text{ }^\circ\text{C}$.

Site	Concentration (mmol g^{-1})	pKa
HA ₁	1.1 ± 0.1^a	4.4 ± 0.2
HA ₂	0.64 ± 0.04	5.8 ± 0.2
HA ₃	0.26 ± 0.08	7.23 ± 0.01
$\sum_{j=1}^3 \text{HA}_j$	2.0 ± 0.2	
HA ₄	0.45 ± 0.07	8.26 ± 0.04
HA ₅	0.46 ± 0.08	9.9 ± 0.2
$\sum_{j=1}^5 \text{HA}_j$	2.9 ± 0.4	

^a Results are the mean of three determinations.

decreased the peak currents (for the same $C_{\text{Hg},T}$) as a consequence of the complexation reaction.

3.4. Interaction between HA and Hg(II)

3.4.1. Properties of the HA

Concentration and pKa of ionizable sites of the HA were determined in medium of $0.020 \text{ mol L}^{-1} \text{ NaNO}_3$ by potentiometric titration using the linear modified Gran functions for data treatment [26]. Five classes of titratable groups fitted the experimental data (Table 2). The total concentration of carboxylic groups was $(2.0 \pm 0.2) \times 10^{-3} \text{ mol g}^{-1}$, corresponding to 69% of the total of $(2.9 \pm 0.4) \times 10^{-3} \text{ mol g}^{-1}$ titratable groups. The titrations with Hg(II) were made using 25.0 mg L^{-1} of HA, so that a total concentration of $72.5 \mu\text{mol L}^{-1}$ of ionizable groups was present in each titration tube. As the initial Hg(II) concentrations varied from 1.0 to $20.0 \mu\text{mol L}^{-1}$ the ligand to metal ratio varied from 72.5 to 3.6 .

3.4.2. Titration of HA with Hg(II) in $0.020 \text{ mol L}^{-1} \text{ NaNO}_3$, pH 6.0

Fig. 5 shows a calibration curve superposed to the titration of a 25.0 mg L^{-1} suspension of HA with $C_{\text{Hg},T}$ from 1.0 to $20 \mu\text{mol L}^{-1}$. The peak potential was plotted for the complexing and non-complexing medium as a function of $C_{\text{Hg},T}$. As the peak potential

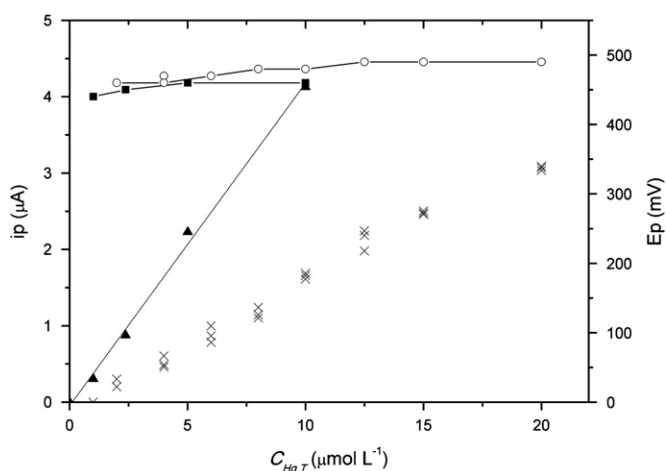


Fig. 5. Variation of peak current (\blacktriangle and \times) and peak potential (\blacksquare and \circ) during titration of non-complexing (\blacksquare and \blacktriangle) and complexing medium (\times and \circ) with Hg(II). The background medium in all solutions was $0.020 \text{ mol L}^{-1} \text{ NaNO}_3$ at pH 6.0. Concentration of HA was 25.0 mg L^{-1} ($72.6 \text{ } \mu\text{mol L}^{-1}$ of ionizable sites). Experiments were made at $25.0 \pm 0.5 \text{ } ^\circ\text{C}$. Measurements were made by injecting $250 \text{ } \mu\text{L}$ of sample at $30 \text{ } \mu\text{L s}^{-1}$, deposition time of 32 s and square wave frequency of 100 Hz.

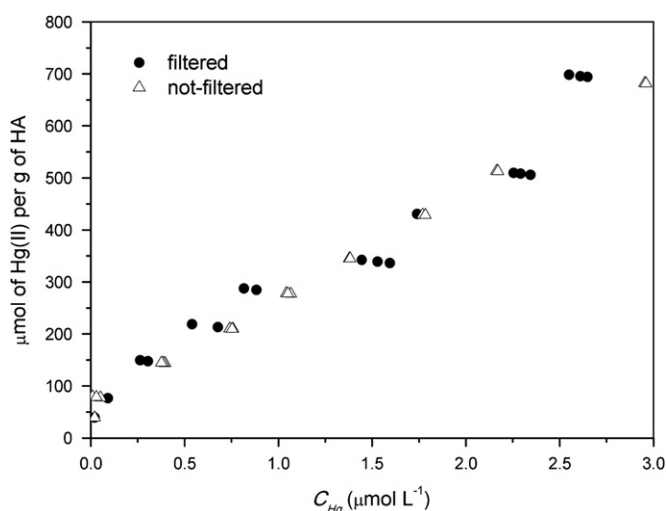


Fig. 6. Adsorption isotherms of Hg(II) obtained from measurements in filtered and non-filtered suspensions of HAs. Experiments were made at $25.0 \pm 0.5 \text{ } ^\circ\text{C}$, in $0.02 \text{ mol L}^{-1} \text{ NaNO}_3$ and pH 6.0 ± 0.1 using a HA concentration of 25.0 mg L^{-1} and $C_{\text{Hg},T} = 1.0, 2.0, 4.0, 6.0, 8.0, 10.0, 12.5, 15.0$ and $20 \text{ } \mu\text{mol L}^{-1}$.

depends on the composition of the stripping medium and in these experiments the stripping step was always made in $0.050 \text{ mol L}^{-1} \text{ HCl}$, no variation of peak potential was expected (Fig. 5), demonstrating the efficiency of the medium exchange.

Adsorption isotherms obtained from measurements made in filtered and non-filtered suspensions of HA were superposed as in Fig. 6. Filtered suspension resulted a Langmuir isotherm up to the $C_{\text{Hg},T}$ of $10 \text{ } \mu\text{mol L}^{-1}$ ($C_{\text{Hg}} \sim 1.5 \text{ } \mu\text{mol L}^{-1}$), but as the $C_{\text{Hg},T}$ increased, an increase in the adsorption was also observed, indicating a cooperative effect. One may infer that this behavior was related to the supramolecular nature of HA, that is, after some loading of Hg(II), structural rearrangements may occur exposing adsorption sites, facilitating the adsorption process. Data of this isotherm fitted to the Langmuir equation, resulting a $Q_{\text{max}} = 537 \pm 30 \text{ } \mu\text{mol g}^{-1}$ (108 mg g^{-1}) and $\log K_L = (3.3 \pm 0.3) \times 10^6 \text{ L mol}^{-1}$ ($r^2 > 0.95$). Data were also fitted by the Freundlich equation, resulting a $1/n$ value of 0.58 ± 0.04 (high heterogeneity of binding sites) and a $K_f = 304 \pm$

$1 \text{ } \mu\text{mol}^{1-1/n} \text{ g}^{-1} \text{ L}^{1/n}$. The value of Q_{max} corresponds to 18% of the total of ionizable sites determined by acid-base titration and to 33.5% of the total of deprotonated sites at pH 6.0. The magnitude of K_L is consistent with values reported for complexation of Hg(II) by carboxylic and phenolic groups [5,40]. The complexation capacity indicates that more than one ionizable site is used for complexation of each Hg(II) and that not all sites are involved in this process, as described by other authors using different speciation techniques [40,41].

The filtered suspension exhibited an almost linear behavior in the range of $C_{\text{Hg},T}$ studied, indicating that the binding energy is independent of the metal loading. Data were not fitted by the Langmuir equation, but fitted well ($r^2 > 0.95$) to the Freundlich model, resulting a $K_f = 275 \pm 1 \text{ } \mu\text{mol}^{1-1/n} \text{ g}^{-1} \text{ L}^{1/n}$ and $1/n = 0.77 \pm 0.02$. Despite of the differences observed in the fitting of the experimental data to the classical Langmuir and Freundlich isotherms, the high degree of overlapping observed for filtered and non-filtered suspensions suggests that the fraction of free plus labile Hg(II) concentrations are independent of the presence colloidal particles of HA. Additionally, it suggests that Hg(II)-containing humic aggregates retained in the $0.20 \text{ } \mu\text{m}$ are either electrochemically inert or very slow diffusing, not contributing to the stripping currents.

3.4.3. Average and differential equilibrium functions

From the computed values of C_{Hg} and the C_L in the HA suspension of $7.26 \times 10^{-5} \text{ mol L}^{-1}$ (considering the abundance of 2.90×10^{-3} of ionizable sites per gram of HA), a range of $\log \theta$ varying from -1.6 to -0.5 was investigated (Fig. 7). In this range of $\log \theta$ the $\log K_{\text{DEF}}$ decreased from 7.0 to 5.3, independently if the measurements were made in filtered or non-filtered suspensions. The heterogeneity parameter (Γ) obtained from the plot of $\log \theta$ vs. $\log K_{\text{DEF}}$ was 0.61 ± 0.03 , which is consistent with the $1/n$ term of the Freundlich equation. The advantage of this approach is that it gives an idea on how the strength of binding decreases with the increase of site occupation [28]. Despite of the range of $\log \theta$ and $\log K_{\text{DEF}}$ studied is typically due to carboxylic and phenolic groups, the value of $\Gamma < 1$ suggests that the heterogeneity may be related to conformational arrangements of the binding sites, as well as the dynamic supramolecular properties of HA as a function of the Hg(II) loading. The $\log \bar{K}$ varied from 4.2 to 3.6, which is consistent with stability constants obtained for complexation of Hg(II) by HAs governed by oxygen containing ligands (carboxylic and phenolic groups) found by potentiometric measurements [5] or by fluorescence quenching [8,9].

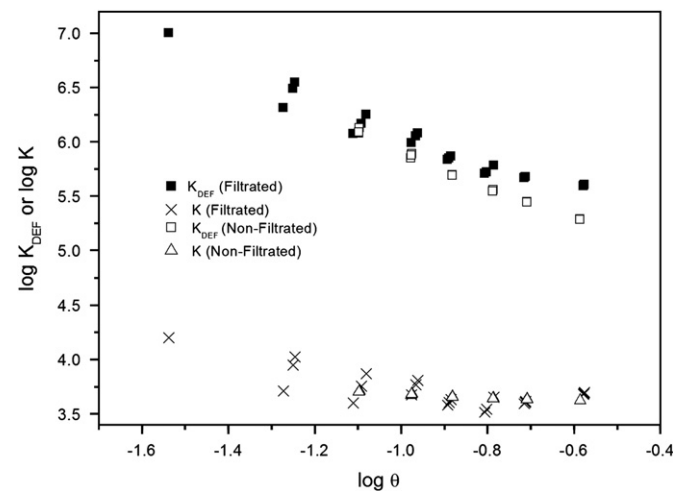


Fig. 7. Plots of $\log K_{\text{DEF}}$ vs. $\log \theta$ obtained from filtered and non-filtered suspensions of HA. All other conditions are as described in legend of Fig. 6.

4. Conclusion

A new SI method to determine dynamic speciation parameters related to the complexation of Hg(II) by HA was developed. The method allows one to make 17 to 35 analyses per hour and uses low cost and portable equipment, with potential for field application, especially considering the use of screen printed electrodes [42] and miniaturized potentiostats. Complexation parameters were obtained from direct peak current measurements without the need of chemometric data treatment of the voltammograms [43]. Different analytical windows can be explored by just changing parameters such as sample volume, flow rate and deposition time from the keyboard of a computer without the need of mechanical or instrumental changes. This is a well known feature of sequential injection systems that can be useful for dynamic speciation studies. In the analytical window explored in the present work, interaction of Hg(II) with carboxylic groups of a commercial HA was studied and the complexation parameters found were compatible with those found by other authors using different analytical techniques.

Acknowledgments

Authors are grateful to Conselho Nacional de Desenvolvimento Científico e Tecnológico (CNPq) for the financial support (Grants 475554/2009-4 and 304178/2009-8). FHN acknowledges a fellowship from Fundação de Amparo à Pesquisa do Estado de São Paulo (FAPESP), process number 2010/04372-1.

References

- [1] J.D. Gasper, G.R. Aiken, J.N. Ryan, *Appl. Geochem.* 22 (2007) 1583–1597.
- [2] A. Piccolo, *Soil Sci.* 166 (2001) 810–832.
- [3] M. Haitzer, G. Aiken, J. Ryan, *Environ. Sci. Technol.* 36 (2002) 3564–3570.
- [4] M. Haitzer, G. Aiken, J. Ryan, *Environ. Sci. Technol.* 37 (2003) 2436–2441.
- [5] Y. Yin, H.E. Allen, C.P. Huang, P.F. Sanders, *Anal. Chim. Acta* 341 (1997) 73–82.
- [6] Q. Wu, S.C. Apte, G.E. Batley, K.C. Bowles, *Anal. Chim. Acta* 350 (1997) 129–134.
- [7] U.L. Skylberg, K. Xia, P.R. Bloom, E.A. Nater, W.F. Bleam, *J. Environ. Qual.* 29 (2000) 855–865.
- [8] X. Lu, R. Jafe, *Water Res.* 35 (2001) 1793–1803.
- [9] C. Xiaoli, L. Guixiang, Z. Xin, H. Yongxia, Z. Youcai, *J. Hazard. Mater.* 209–210 (2012) 59–66.
- [10] C.H. Langborg, C. Tseng, W.F. Fitzgerald, P.H. Balcom, C.R. Hammerschmidt, *Environ. Sci. Technol.* 37 (2003) 3316–3322.
- [11] R.M. Town, M. Fillela, *Aquat. Sci.* 62 (2000) 252–295.
- [12] L. Sigg, F. Black, J. Buffle, J. Cao, R. Cleven, W. Davinso, J. Galceran, P. Gunkel, E. Kalis, D. Kistler, M. Martin, S. Noel, Y. Nur, N. Odzak, J. Puy, W. van Riemsdijk, E. Temminghof, M.L. Tercier-Waeber, S. Toepperwien, R.M. Town, E. Unsworth, K.W. Warken, L. Weng, H. Xue, H. Zhang, *Environ. Sci. Technol.* 40 (2006) 1934–1941.
- [13] J. Ruzicka, G.D. Marshall, *Anal. Chim. Acta* 237 (1990) 329–343.
- [14] A. Ivaska, W.W. Kubiak, *Talanta* 44 (1997) 713–723.
- [15] C.L. da Silva, J.C. Masini, *Fresenius J. Anal. Chem.* 367 (2000) 284–290.
- [16] A.C. Vieira dos Santos, J.C. Masini, *Anal. Bioanal. Chem.* 385 (2006) 1538–1544.
- [17] W.W. Kubiak, R.M. Laitonen, A. Ivaska, *Talanta* 53 (2001) 1211–1219.
- [18] F. Okcu, H. Ertas, F. Nil Ertas, *Talanta* 75 (2008) 442–446.
- [19] J.P. Metters, R.O. Kadara, C.E. Banks, *Analyst* 136 (2011) 1067–1076.
- [20] M. Li, Y.T. Li, D.W. Li, Y.T. Long, *Anal. Chim. Acta* 734 (2012) 31–44.
- [21] L. Laschi, I. Palchetti, M. Mascini, *Sensors Actuators B* 114 (2006) 460–465.
- [22] P. Danwanichakul, D. Danwanichakul, *Eur. J. Sci. Res.* 36 (2009) 363–375.
- [23] J.P. Pinheiro, A.M. Mota, H.P. van Leeuwen, *Anal. Chim. Acta* 284 (1994) 525–537.
- [24] H.P. van Leeuwen, R. Cleven, J. Buffle, *Pure Appl. Chem.* 61 (1989) 255–274.
- [25] M.G. Bugarin, A.M. Mota, J.P. Pinheiro, M.L.S. Gonçalves, *Anal. Chim. Acta* 294 (1994) 271–281.
- [26] J.C. Masini, G. Abate, E.C. Lima, M.S. Nakamura, J. Lichtig, H.R. Nakamura, *Anal. Chim. Acta* 364 (1998) 223–233.
- [27] G. Abate, J.C. Masini, *Org. Geochem.* 33 (2002) 1171–1182.
- [28] R.S. Altmann, J. Buffle, *Geochim. Cosmochim. Acta* 52 (1988) 1505–1519.
- [29] E. Pinilla Gil, P. Ostapczuk, *Anal. Chim. Acta* 293 (1994) 55–65.
- [30] A. Giacomino, O. Abollino, M. Malandrino, E. Mentasti, *Talanta* 75 (2008) 266–273.
- [31] A. Mandil, L. Idrissi, A. Amine, *Microchim. Acta* 170 (2010) 299–305.
- [32] E. Bernalte, C.M. Sánchez, E.P. Gil, *Anal. Chim. Acta* 689 (2011) 60–64.
- [33] L.B.O. dos Santos, M.S.P. Silva, J.C. Masini, *Anal. Chim. Acta* 528 (2005) 21–27.
- [34] M. Fillela, W. Hummel, *Accred. Qual. Assur.* 16 (2011) 215–223.
- [35] E.M. Richter, M.A. Augelli, G.H. Kume, R.N. Mioshi, L. Angnes, *Fresenius J. Anal. Chem.* 366 (2000) 444–448.
- [36] M.A. Augelli, R.A.A. Munoz, E.M. Richter, A. Gouveia Jr, L. Angnes, *Electroanalysis* 17 (2005) 755–761.
- [37] Y. Bonfil, M. Brand, E. Kirova-Eisner, *Anal. Chim. Acta* 424 (2000) 65–76.
- [38] A. Walcarus, M. Etienne, C. Delacote, *Anal. Chim. Acta* 508 (2004) 87–98.
- [39] L. Xiao, W. Dietze, F. Nyasulu, B.A.F. Mibeck, *Anal. Chem.* 78 (2006) 5172–5178.
- [40] S.S. Lee, K.L. Naggy, C. Park, P. Fenter, *Environ. Sci. Technol.* 43 (2009) 5295–5300.
- [41] R.T. Drexel, M. Haitzer, J.N. Ryan, G.R. Aiken, K.L. Naggy, *Environ. Sci. Technol.* 36 (2002) 4058–4064.
- [42] C. Parat, A. Schneider, A. Castetbon, M. Potin-Gautier, *Anal. Chim. Acta* 688 (2011) 156–162.
- [43] E. Chekmeneva, J.M. Díaz-Cruz, C. Ariño, M. Esteban, *J. Electroanal. Chem.* 629 (2009) 169–179.